



Title	Influence of off-stoichiometry on magnetoresistance characteristics of Co ₂ MnSi/Ag-based current-perpendicular-to-plane spin valves
Author(s)	Inoue, Masaki; Hu, Bing; Moges, Kidist; Inubushi, Kazuumi; Nakada, Katsuyuki; Yamamoto, Masafumi; Uemura, Tetsuya
Citation	Applied physics letters, 111(8), 82403 https://doi.org/10.1063/1.5000244
Issue Date	2017-08-21
Doc URL	http://hdl.handle.net/2115/71320
Rights	This article may be downloaded for personal use only. Any other use requires prior permission of the author and AIP Publishing. The following article appeared in Appl. Phys. Lett. 111, 082403 (2017); doi: 10.1063/1.5000244, and may be found at http://dx.doi.org/10.1063/1.5000244 .
Type	article
File Information	1.5000244.pdf



[Instructions for use](#)

Influence of off-stoichiometry on magnetoresistance characteristics of $\text{Co}_2\text{MnSi}/\text{Ag}$ -based current-perpendicular-to-plane spin valves

Masaki Inoue, Bing Hu, Kidist Moges, Kazuumi Inubushi, Katsuyuki Nakada, Masafumi Yamamoto, and Tetsuya Uemura

Citation: *Appl. Phys. Lett.* **111**, 082403 (2017); doi: 10.1063/1.5000244

View online: <http://dx.doi.org/10.1063/1.5000244>

View Table of Contents: <http://aip.scitation.org/toc/apl/111/8>

Published by the [American Institute of Physics](#)

Articles you may be interested in

[Spin diffusion length of Permalloy using spin absorption in lateral spin valves](#)

Applied Physics Letters **111**, 082407 (2017); 10.1063/1.4990652

[Spin-orbit torque induced magnetization switching in Co/Pt multilayers](#)

Applied Physics Letters **111**, 102402 (2017); 10.1063/1.5001171

[Frequency shift keying by current modulation in a MTJ-based STNO with high data rate](#)

Applied Physics Letters **111**, 082401 (2017); 10.1063/1.4994892

[Exchange coupling of a perpendicular ferromagnet to a half-metallic compensated ferrimagnet via a thin hafnium interlayer](#)

Applied Physics Letters **111**, 102403 (2017); 10.1063/1.5001172

[Bias dependence of spin transfer torque in \$\text{Co}_2\text{MnSi}\$ Heusler alloy based magnetic tunnel junctions](#)

Applied Physics Letters **110**, 172403 (2017); 10.1063/1.4981388

[Enhancement of \$L_{21}\$ order and spin-polarization in \$\text{Co}_2\text{FeSi}\$ thin film by substitution of Fe with Ti](#)

Applied Physics Letters **110**, 242401 (2017); 10.1063/1.4985237



5 Electronic Measurement Pitfalls to Avoid

Get the whitepaper

Influence of off-stoichiometry on magnetoresistance characteristics of Co₂MnSi/Ag-based current-perpendicular-to-plane spin valves

Masaki Inoue,¹ Bing Hu,¹ Kidist Moges,¹ Kazuumi Inubushi,² Katsuyuki Nakada,² Masafumi Yamamoto,¹ and Tetsuya Uemura^{1,a)}

¹Division of Electronics for Informatics, Graduate School of Information Science and Technology, Hokkaido University, Sapporo 060-0814, Japan

²Technical Center, TDK Corporation, Ichikawa 272-8558, Japan

(Received 3 April 2017; accepted 12 August 2017; published online 24 August 2017)

The influence of off-stoichiometry of Co₂MnSi (CMS) spin sources on giant magnetoresistance characteristics was investigated for CMS/Ag-based current-perpendicular-to-plane spin valves prepared with various Mn compositions α in Co₂Mn _{α} Si_{0.82} electrodes. The magnetoresistance ratio of the prepared CMS/Co₅₀Fe₅₀ (CoFe) (1.1 nm)/Ag/CoFe (1.1)/CMS spin valves systematically increased with α from 11.4% for Mn-deficient $\alpha=0.62$ to 20.7% for Mn-rich $\alpha=1.45$ at 290 K. This result suggests that increasing α from a Mn-deficient to Mn-rich value increases the spin polarization by suppressing Co_{Mn} antisites harmful to the half-metallicity. Thus, our results demonstrate that appropriately controlling the film composition toward a Mn-rich one is highly effective for enhancing the half-metallicity of CMS in CMS-based spin valves, as it is in CMS-based magnetic tunnel junctions. *Published by AIP Publishing.* [<http://dx.doi.org/10.1063/1.5000244>]

Spintronic devices, which exploit spin-dependent electron transport phenomena, have attracted much interest because of their potential advantages of nonvolatility, decreased power consumption, and reconfigurable logic function capabilities.^{1,2} Co-based Heusler alloys (Co₂YZ, where Y is usually a transition metal and Z is a main group element) are promising ferromagnetic electrode materials for spintronic devices, including magnetic tunnel junctions (MTJs),^{3–16} current-perpendicular-to-plane (CPP) giant magnetoresistance (GMR) devices,^{17–28} and for spin injection into semiconductors.^{29–33} This is because many of them are theoretically predicted to have half-metallicity, which is characterized by an energy gap for one spin direction, which in turn provides complete spin polarization at the Fermi level (E_F),^{34–37} and because they have relatively high Curie temperatures, well above room temperature (RT).³⁸ To take full advantage of the half-metallic character of Co-based Heusler alloys, it is important to clarify the effect of structural defects on the half-metallicity. Picozzi *et al.* theoretically predicted that Co_{Mn} antisites, where a Mn site is replaced by Co, in Co₂MnSi (CMS) cause minority-spin in-gap states at E_F and thus are detrimental to the half-metallicity of CMS.³⁹ We have systematically investigated the effect of off-stoichiometry on the half-metallicity of CMS, Co₂MnGe, and Co₂(Mn,Fe)Si (CMFS) by using various experimental approaches, including the tunneling magnetoresistance (TMR) ratios of MTJs,^{7–10,14,15} the saturation magnetization,^{10,15} the surface spin polarization,⁴⁰ the magnetic states as investigated by x-ray absorption spectroscopy and x-ray magnetic circular dichroism,^{41–43} and the electronic states as investigated through spin-resolved low-energy and hard x-ray photoelectron spectroscopy.^{44–46} These experimental studies, along with first-principles calculations, demonstrated that Co_{Mn} antisites induced by a Mn-deficient composition (the Mn composition $\alpha < 2 - \beta'$ in the composition expression of Co₂Mn _{α} Si _{β'})

are indeed detrimental to the half-metallicity of CMS. Furthermore, it was shown that harmful Co_{Mn} antisites can be suppressed and half-metallicity was enhanced by preparing CMS thin films with a Mn-rich composition.^{7–10} It was also shown that (Mn + Fe)-rich compositions are critical to suppressing these harmful antisites and to retaining the half-metallic electronic states for Co₂(Mn,Fe)Si quaternary alloys.^{14,15} In light of these findings, we demonstrated giant TMR ratios of 1995% at 4.2 K and 354% at 290 K for CMS/MgO/CMS MTJs (CMS MTJs) with Mn-rich CMS electrodes⁹ and up to 2610% at 4.2 K and 429% at 290 K for CMFS/MgO/CMFS MTJs (CMFS MTJs) with Mn-rich, lightly Fe-doped CMFS electrodes.^{14,15}

For Heusler alloy-based CPP-GMR devices, Li *et al.* reported an enhancement of the MR ratio in Mn-rich Co₂Mn(Ge,Ga) (CMGG).²⁸ However, the investigation in Ref. 28 on the Mn composition dependence of the MR characteristics was limited to two typical compositions, one having a Co-rich composition of Co₂Mn_{0.97}(Ge_{0.63}Ga_{0.24}) and the other having a Mn-rich composition of Co₂Mn_{1.24}(Ge_{0.76}Ga_{0.31}).

The purpose of the present study was to clarify the influence of off-stoichiometry in CMS films on the MR characteristics of CPP spin valves. To do this, we fabricated CPP-GMR devices with an exchange-biased spin-valve structure having CMS electrodes with various Mn compositions, α , and an Ag spacer and systematically investigated the influence of α on the MR characteristics. We prepared these CPP spin valves with ultrathin Co₅₀Fe₅₀ (CoFe) thin layers inserted at the upper and lower interfaces in the CMS/Ag/CMS trilayer.

The fabricated CPP-spin-valve layer structures were as follows: (from the substrate side) MgO buffer (10 nm)/CoFe (10)/Ag (100)/CoFe (10)/CMS lower electrode (3)/CoFe (t_{CoFe})/Ag spacer (5)/CoFe (t_{CoFe})/CMS upper electrode (3)/CoFe (1.1)/Ir₂₂Mn₇₈ (10)/Ru cap (5) with Co₂Mn _{α} Si_{0.82} electrodes, grown on MgO(001) substrates [Fig. 1(a)], where t_{CoFe} represents the thickness of the ultrathin CoFe layers

^{a)}E-mail: uemura@ist.hokudai.ac.jp

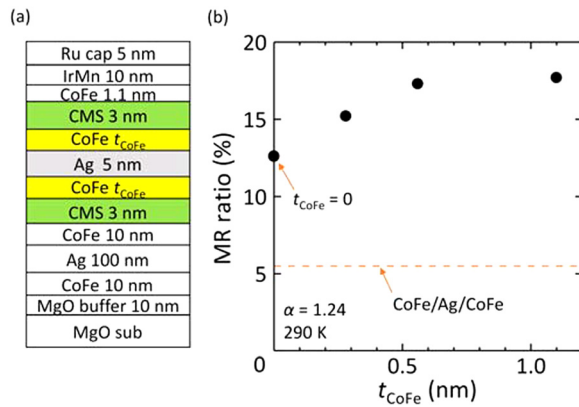


FIG. 1. (a). Layer structure of the fabricated CPP spin valves consisting of (from the substrate side) MgO buffer (10 nm)/ $\text{Co}_{50}\text{Fe}_{50}$ (CoFe) (10)/Ag (100)/CoFe (10)/ Co_2MnSi (CMS) lower electrode (3)/CoFe (t_{CoFe})/Ag spacer (5)/CoFe (t_{CoFe})/CMS upper electrode (3)/CoFe (1.1)/ $\text{Ir}_{22}\text{Mn}_{78}$ (10)/Ru cap (5), grown on MgO(001) substrates. (b) MR ratio at 290 K for series-A spin valves [CMS/CoFe (t_{CoFe})/Ag/CoFe (t_{CoFe})/CMS] with Mn composition, α , of 1.24 ($\text{Co}_2\text{Mn}_{1.24}\text{Si}_{0.82}$) electrodes as a function of thickness of ultrathin CoFe layers inserted at the interfaces, t_{CoFe} . The dashed line indicates the MR ratio of identically prepared CoFe (10 nm)/Ag (5)/CoFe (3) spin valve, which was distinctly lower than that of the original CMS/Ag/CMS, indicating that the spin polarization of CMS with $\alpha = 1.24$ was higher than that of CoFe. The MR ratio is defined as $(R_{\text{AP}} - R_{\text{P}})/(R_{\text{P}} - R_{\text{C}})$ in which the influence of the contact resistance R_{C} is corrected.

inserted at the interfaces. We first investigated the effect of inserting ultrathin CoFe layers at the interfaces in the CMS/Ag/CMS trilayer on the MR ratio, aiming at enhancing it. To do this, we prepared the CPP spin valves with $\alpha = 1.24$, corresponding to a slightly (Mn + Si)-rich composition in $\text{Co}_2\text{Mn}_\alpha\text{Si}_{1-\alpha}$ electrodes, by varying t_{CoFe} from 0 to 1.1 nm (series-A spin valves). Given the result that t_{CoFe} of 1.1 nm provided the highest MR ratio in series-A spin valves as described below, we then investigated the influence of off-stoichiometry on the MR characteristics by varying α in $\text{Co}_2\text{Mn}_\alpha\text{Si}_{1-\alpha}$ electrodes ranging from $\alpha = 0.62$ to 1.45 while fixing the value of t_{CoFe} ($=1.1$ nm) (series-B spin valves). Each layer was successively deposited in an ultrahigh vacuum chamber with a base pressure of about 5×10^{-8} Pa. Epitaxial growth of each layer was confirmed by making *in-situ* reflection high-energy electron diffraction (RHEED) observations. The procedure of preparing the CMS electrodes was the same as for the CMS/MgO MTJs.^{7,9} The film composition of the prepared CMS film was determined through an inductively coupled plasma analysis with an accuracy of 2%–3% for each element, except for Si, for which the accuracy was 5%. Just after the deposition of the CMS upper electrodes, the layer structure was *in situ* annealed at 500 °C for series-A spin valves and at 550 °C for series-B spin valves both for 15 min. The post-deposition annealing temperature (T_{a}) for series-B spin valves was optimized to be 550 °C by investigating the T_{a} dependence of the MR ratio for the CPP spin valves with $\alpha = 1.12$ and $t_{\text{CoFe}} = 1.1$ nm. We fabricated CPP spin valves with these layer structures by electron beam lithography and Ar ion milling. The sizes of the prepared junctions were determined by scanning electron microscopy observations for nanostructured pillars, which were ones just after the Ar ion milling conducted using a resist mask. The junction sizes reported in this letter are the actual measured values. The MR characteristics are reported for spin

valves having relatively small junction sizes of 140×75 and 100×50 nm. The parasitic contact resistance values R_{C} were determined by plotting the junction resistances R_{P} at 290 K as a function of A^{-1} for the prepared junctions having relatively large junction sizes ranging from 525×320 to 140×75 nm, where A is the junction area. After fabrication, the devices were annealed *ex situ* at 325 °C under a magnetic field of 5 kOe to apply an exchange bias effect to the upper electrode. The MR characteristics were investigated using a dc four-probe method from 4.2 K to 290 K. We defined the MR ratio as $(R_{\text{AP}} - R_{\text{P}})/(R_{\text{P}} - R_{\text{C}})$, which is the experimental MR ratio corrected for the influence of R_{C} , where R_{P} and R_{AP} are the junction resistances for the parallel and antiparallel magnetization configurations between the upper and lower electrodes.

First, we describe the effect of inserting the ultrathin CoFe layers at the interfaces in the CMS/Ag/CMS trilayer on the MR ratio. Figure 1(b) plots the MR ratio at 290 K for series-A spin valves [CMS/CoFe (t_{CoFe})/Ag/CoFe (t_{CoFe})/CMS] with $\alpha = 1.24$ as a function of t_{CoFe} ranging from $t_{\text{CoFe}} = 0$ (corresponding to the $\alpha = 1.24$ CMS/Ag/CMS spin valve without inserted CoFe layers) to $t_{\text{CoFe}} = 1.1$ nm, along with the MR ratio of an identically fabricated CoFe (10 nm)/Ag (5)/CoFe (3) spin valve. The MR ratio of 12.5% for the original $\alpha = 1.24$ CMS/Ag/CMS spin valve without the inserted layers was significantly higher than the 5.5% for the identically prepared CoFe/Ag/CoFe spin valve, indicating that the spin polarization of the $\alpha = 1.24$ CMS electrodes as spin sources in the original CMS/Ag/CMS spin valves was distinctly higher than that of the CoFe electrodes in the reference CoFe/Ag/CoFe spin valve. Notably, the MR ratio of CMS/Ag/CMS spin valves was enhanced by inserting ultrathin CoFe layers at the interfaces and increased with an increase in t_{CoFe} up to 0.56 and 1.1 nm, resulting in a significantly enhanced MR ratio of 17.7% for t_{CoFe} of 1.1 nm compared with that of 12.5% for the original $\alpha = 1.24$ CMS/Ag/CMS. It is obvious that the CMS electrodes worked as spin sources in CoFe-inserted CMS/Ag/CMS because of the distinctly lower MR ratio of the CoFe/Ag/CoFe spin valve compared with the original CMS/Ag/CMS. Thus, the enhancement of the MR ratio caused by inserting ultrathin CoFe layers should be ascribed to the interface modification, although further study is needed to clarify the origin. Similar enhancement of the MR ratio due to inserting ultrathin CoFe layers was reported previously in $\text{Co}_2\text{Mn}(\text{Ga}_{0.5}\text{Sn}_{0.5})/\text{Ag}$ -based pseudo spin valves.²¹

We now describe how the MR characteristics of series-B spin valves [CMS/CoFe (1.1 nm)/Ag/CoFe (1.1)/CMS] depended on α in $\text{Co}_2\text{Mn}_\alpha\text{Si}_{1-\alpha}$ electrodes. A typical MR curve at 290 K for a series-B spin valve with Mn-rich ($\alpha = 1.45$) CMS electrodes is shown in Fig. 2(a). The junction area A was 100×50 nm². The curve shows clear MR characteristics with an MR ratio of 20.7%. $R_{\text{P}} \cdot A$ and $\Delta R \cdot A$ were 15.0 m $\Omega \cdot \mu\text{m}^2$ and 3.1 m $\Omega \cdot \mu\text{m}^2$, respectively, where $\Delta R = R_{\text{AP}} - R_{\text{P}}$. Figure 2(b) shows the MR ratio of series-B spin valves at 290 K as a function of α ranging from $\alpha = 0.62$ to 1.45. Most importantly, the MR ratio significantly increased from 11.4% for the Mn-deficient composition ($\alpha = 0.62$) to 20.7% for the Mn-rich ($\alpha = 1.45$). This result suggests a continuous increase in the spin polarization of the CMS electrodes with increasing α from a Mn-deficient to Mn-rich composition, which can be understood in terms of the suppression of Co_{Mn} antisites by Mn-rich

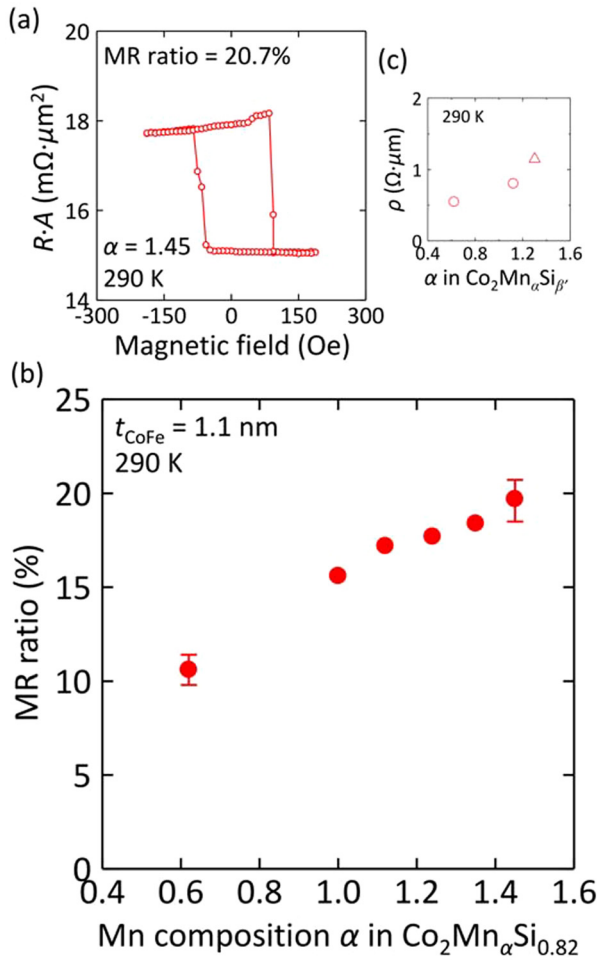


FIG. 2. (a) Typical MR curve at 290 K for a series-B spin valve [CMS/CoFe (1.1 nm)/Ag/CoFe (1.1)/CMS] with Mn-rich ($\alpha = 1.45$) CMS electrodes and (b) MR ratio of series-B spin valves at 290 K as a function of Mn composition, α , in $\text{Co}_2\text{Mn}_\alpha\text{Si}_{0.82}$ electrodes ranging from $\alpha = 0.62$ to 1.45. (c) Mn-composition dependence of the resistivity, ρ , of off-stoichiometric Co_2MnSi thin films at 290 K in $\text{Co}_2\text{Mn}_\alpha\text{Si}_{\beta'}$ ($\beta' = 0.82$ or 0.90). The ρ values of two samples with $\alpha = 0.62$ and 1.12 in $\text{Co}_2\text{Mn}_\alpha\text{Si}_{0.82}$ (open circles), and a sample with $\alpha = 1.30$ in $\text{Co}_2\text{Mn}_\alpha\text{Si}_{0.90}$ (open triangle) are shown, where $\alpha + \beta' < 2$ and $\alpha + \beta' > 2$ in $\text{Co}_2\text{Mn}_\alpha\text{Si}_{\beta'}$ correspond to (Mn + Si)-deficient and (Mn + Si)-rich compositions, respectively.

compositions. Figure 2(c) shows how the resistivity, ρ , of off-stoichiometric Co_2MnSi thin films at 290 K varied with α in $\text{Co}_2\text{Mn}_\alpha\text{Si}_{\beta'}$ ($\beta' = 0.82$ or 0.90). It increased with increasing α from $\rho = 0.55 \Omega \cdot \mu\text{m}$ for (Mn+Si)-deficient $\text{Co}_2\text{Mn}_{0.62}\text{Si}_{0.82}$ to $\rho = 1.1 \Omega \cdot \mu\text{m}$ for (Mn + Si)-rich $\text{Co}_2\text{Mn}_{1.30}\text{Si}_{0.90}$. The influence of ρ of CMS films on the experimental MR ratio will be discussed below.

Figure 3(a) shows typical temperature (T) dependences of R_{AP} and R_{P} for a series-B spin valve with $\alpha = 1.45$. Furthermore, Fig. 3(b) shows the T dependence of the measured MR ratios, defined as $(R_{\text{AP}} - R_{\text{P}})/R_{\text{P}}$, in which the influence of R_{c} is not corrected, of series-B spin valves with $\alpha = 0.62, 1.0$, and 1.45 (we describe the measured MR ratio as the MR ratio regarding its T dependence). As shown in Fig. 3(a), R_{P} decreased almost monotonically with decreasing T from 290 K to 4.2 K. On the other hand, R_{AP} decreased slightly with decreasing T for a T range from 290 K to a certain temperature, T_{M} , of about 220 K for the $\alpha = 1.45$ spin valve, and then it decreased rapidly for a T range below T_{M} . This behavior resulted in that the MR ratio of the $\alpha = 1.45$

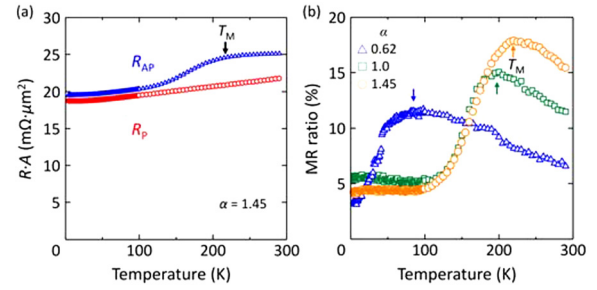


FIG. 3. (a) Temperature dependence of R_{AP} and R_{P} for a series-B spin valve [CMS/CoFe (1.1 nm)/Ag/CoFe (1.1)/CMS] with Mn-rich ($\alpha = 1.45$) CMS electrodes and (b) T dependence of the measured MR ratio, defined as $(R_{\text{AP}} - R_{\text{P}})/R_{\text{P}}$ in which the influence of R_{c} is not corrected, for series-B spin valves with $\alpha = 0.62, 1.0$, and 1.45.

spin valve increased with decreasing T in a T range from 290 K to T_{M} while it quickly decreased with decreasing T for a T range from T_{M} of 220 K to about 100 K [Fig. 3(b)] due to the significant decrease in R_{AP} .

The increase in the MR ratio as decreasing T from 290 K to T_{M} of 220 K is as would be expected from spin-dependent transport in GMR devices. In more detail, an increase in the spin polarization of the CMS electrodes and decreasing spin-flip transport via thermally excited magnons in spin-valve trilayers with decreasing T lead to a decrease in R_{P} and an increase in R_{AP} as T decreases, while a decrease in the resistivities of the metallic layers involved in the nanopillar, including the Ru cap layer to the CMS lower electrode, with decreasing T due to the suppression of phonon scattering leads to a decrease in both R_{P} and R_{AP} . These factors lead to a more weak decrease in R_{AP} as T decreases compared with R_{P} for the T range from 290 K to T_{M} .

On the other hand, the quick decrease in the MR ratio below T_{M} is unusual. An anomalous decrease in the MR ratio was previously reported for CMS/Ag/CMS spin valves and pseudo spin valves^{20,22,23} and CMFS/Ag/CMFS pseudo spin valves,²⁴ and two possible origins, both of which are related to Mn diffusion from CMS into the Ag spacer, were proposed: One is the presence of a bi-quadratic interlayer exchange coupling between the upper and lower CMS via diffused Mn;²² the second is formation of a spin-glass state of diffused Mn, resulting in a reduction in the spin diffusion length of the Ag spacer.²³ As shown in Fig. 3(b), the characteristic temperature T_{M} [indicated by arrows in Fig. 3(b)] increased with increasing α , resulting in the extension of the range in which the anomalous temperature dependence of the MR ratio was observed, as α increased. This result suggests possible origins related to Mn diffusion into the Ag spacer, as discussed in Refs. 22 and 23.

Now let us discuss the influence of off-stoichiometry for Co_2MnSi films on the MR characteristics. In general, the MR ratio of CPP spin valves depends on not only the bulk spin asymmetry coefficient β of a ferromagnet (equivalent to the spin polarization at E_{F}) but also several other factors such as the interface spin asymmetry coefficient γ , the interface resistance per area (r_{b}), and the resistivity (ρ) and spin diffusion length (l_{sf}) of each layer.⁴⁷ For series-B spin valves, the interfacial structure between the ferromagnet and the Ag spacer was fixed by inserting an ultrathin CoFe layer

at both interfaces. Then, it could be assumed that γ and r_b are constant against a change in the Mn composition. On the other hand, β would increase with increasing α , which has been demonstrated in the various experiments and first-principles calculations, including ones on the giant TMR ratios in CMS/MgO-based MTJs,^{7–10} as described in the introduction. Moreover, ρ for the CMS also increased with increasing α , as shown in Fig. 2(c). The intrinsic MR ratio, $(\text{MR ratio})_{\text{int}}$, of a CPP GMR nanopillar is given by

$$(\text{MR ratio})_{\text{int}} = \frac{\Delta R \cdot A}{(R_P \cdot A)_{\text{int}}}, \quad (1)$$

where $(R_P \cdot A)_{\text{int}}$ is the intrinsic resistance-area product of an F/N/F nanopillar for the parallel magnetization configuration. According to the Valet-Fert model,⁴⁷ $\Delta R \cdot A$ for $t_N \ll l_{\text{sf}}^{(\text{N})}$ and $t_F \gg l_{\text{sf}}^{(\text{F})}$ is given by

$$\begin{aligned} \Delta R \cdot A &= 2 \left(r_{\text{SI}}^{(\text{AP})} - r_{\text{SI}}^{(\text{P})} \right) \\ &= 2\rho_{\text{F}} l_{\text{sf}}^{(\text{F})} \frac{\beta^2}{1 - \beta^2} + 2r_b \frac{\gamma^2}{1 - \gamma^2} - 2r_{\text{SI}}^{(\text{P})}, \end{aligned} \quad (2)$$

and $(R_P \cdot A)_{\text{int}}$ is given by

$$(R_P \cdot A)_{\text{int}} = 2\rho_{\text{F}} t_{\text{F}} + \rho_{\text{N}} t_{\text{N}} + 2r_b + 2r_{\text{SI}}^{(\text{P})}, \quad (3)$$

where $r_{\text{SI}}^{(\text{AP})}$ and $r_{\text{SI}}^{(\text{P})}$ are the interface resistances per area arising from the spin accumulation for the parallel and anti-parallel configurations, ρ_{F} (ρ_{N}) and t_{F} (t_{N}) are the resistivity and the thickness for the ferromagnetic electrode (the normal metal spacer), and $r_{\text{SI}}^{(\text{P})}$ for $r_b < \rho_{\text{N}} t_{\text{N}}$ is given by $r_{\text{SI}}^{(\text{P})} = \rho_{\text{N}} t_{\text{N}} \beta^2 / 2$. Because the term of $2\rho_{\text{F}} l_{\text{sf}}^{(\text{F})}$ for the Co_2MnSi electrodes is much larger than that of $\rho_{\text{N}} t_{\text{N}}$ for the Ag spacer and by assuming an r_b smaller than $\rho_{\text{N}} t_{\text{N}}$, it is suggested that the dominant term in Eq. (3) is $2\rho_{\text{F}} t_{\text{F}}$. Similarly, the first term in Eq. (2) is the dominant term for $\Delta R \cdot A$ because r_b is much smaller than $\rho_{\text{F}} l_{\text{sf}}^{(\text{F})}$ if r_b is smaller than $\rho_{\text{N}} t_{\text{N}}$ ($\rho_{\text{N}} t_{\text{N}}$ for the Ag spacer is much smaller than $\rho_{\text{F}} l_{\text{sf}}^{(\text{F})}$ for the Co_2MnSi electrodes). Accordingly, the above equations (1) to (3) indicate that the intrinsic MR ratio is independent of ρ_{F} and increases with increasing β .

Next, we consider the influence of the external resistance, R_{ext} , involved in a nanopillar on the MR ratio. Although we subtracted the parasitic resistance outside the nanopillar, R_{c} , from R_{P} , $R_{\text{P}} - R_{\text{c}}$ still contains R_{ext} arising from the IrMn and Ru layers involved in the nanopillar. The experimental MR ratio, $(\text{MR ratio})_{\text{exp}}$, in this study is thus expressed as

$$\begin{aligned} (\text{MR ratio})_{\text{exp}} &= \frac{\Delta R \cdot A}{(R_P \cdot A)_{\text{exp}}} = \frac{\Delta R \cdot A}{(R_P \cdot A)_{\text{int}} + R_{\text{ext}} \cdot A} \\ &= (\text{MR ratio})_{\text{int}} \frac{(R_P \cdot A)_{\text{int}}}{(R_P \cdot A)_{\text{int}} + R_{\text{ext}} \cdot A}. \end{aligned} \quad (4)$$

As shown in Eq. (4), $(\text{MR ratio})_{\text{exp}}$ is lower than $(\text{MR ratio})_{\text{int}}$ by a factor f equal to $(R_P \cdot A)_{\text{int}} / \{(R_P \cdot A)_{\text{int}} + R_{\text{ext}} \cdot A\}$ due to $(R_{\text{ext}} \cdot A)$ involved in f . Note that the factor f increases with increasing ρ_{F} because of the $\rho_{\text{F}} t_{\text{F}}$ term in $(R_P \cdot A)_{\text{int}}$ [Eq. (3)] for a constant value of R_{ext} . This would result in an increase

in $(\text{MR ratio})_{\text{exp}}$ because of the extrinsic origin. Although a quantitative evaluation of this extrinsic effect on the increase in the $(\text{MR ratio})_{\text{exp}}$ is difficult at present because R_{ext} has not been separated, a rough estimate indicated that the extrinsic effect due to the increased f was not enough to explain the increase in the $(\text{MR ratio})_{\text{exp}}$ with increasing α . These considerations also indicate that the increase in β with increasing Mn composition played a significant role in increasing the MR ratio.

In summary, we fabricated CPP spin valves having CMS electrodes and investigated the influence of the Mn composition α in $\text{Co}_2\text{Mn}_x\text{Si}_{0.82}$ electrodes on the magnetoresistance characteristics. The MR ratio significantly increased from 11.4% to 20.7% at 290 K with increasing α from 0.62 to 1.45. This result suggests a continuous increase in the bulk spin polarization with increasing α from a Mn-deficient to Mn-rich one. We thus demonstrated that appropriately controlling the film composition toward a Mn-rich one is highly effective for enhancing the half-metallicity of CMS in CMS-based spin valves as it is in MTJs.

This work was partly supported by the Japan Society for the Promotion of Science (KAKENHI: Grant Nos. 25286039, 15K13960, 16K04872, and 17H03225).

¹S. A. Wolf, D. D. Awschalom, R. A. Buhrman, J. M. Daughton, S. von Molnár, M. L. Roukes, A. Y. Chtchelkanova, and D. M. Treger, *Science* **294**, 1488 (2001).

²I. Žutić, J. Fabian, and S. Das Sarma, *Rev. Mod. Phys.* **76**, 323 (2004).

³K. Inomata, S. Okamura, R. Goto, and N. Tezuka, *Jpn. J. Appl. Phys., Part 2* **42**, L419 (2003).

⁴S. Kämmerer, A. Thomas, A. Hütten, and G. Reiss, *Appl. Phys. Lett.* **85**, 79 (2004).

⁵Y. Sakuraba, M. Hattori, M. Oogane, Y. Ando, H. Kato, A. Sakuma, T. Miyazaki, and H. Kubota, *Appl. Phys. Lett.* **88**, 192508 (2006).

⁶T. Ishikawa, T. Marukame, H. Kijima, K.-i. Matsuda, T. Uemura, M. Arita, and M. Yamamoto, *Appl. Phys. Lett.* **89**, 192505 (2006).

⁷T. Ishikawa, H.-x. Liu, T. Taira, K.-i. Matsuda, T. Uemura, and M. Yamamoto, *Appl. Phys. Lett.* **95**, 232512 (2009).

⁸M. Yamamoto, T. Ishikawa, T. Taira, G.-f. Li, K.-i. Matsuda, and T. Uemura, *J. Phys.: Condens. Matter* **22**, 164212 (2010).

⁹H.-x. Liu, Y. Honda, T. Taira, K.-i. Matsuda, M. Arita, T. Uemura, and M. Yamamoto, *Appl. Phys. Lett.* **101**, 132418 (2012).

¹⁰G.-f. Li, Y. Honda, H.-x. Liu, K.-i. Matsuda, M. Arita, T. Uemura, M. Yamamoto, Y. Miura, M. Shirai, T. Saito, F. Shi, and P. M. Voyles, *Phys. Rev. B* **89**, 014428 (2014).

¹¹N. Tezuka, N. Ikeda, F. Mitsuhashi, and S. Sugimoto, *Appl. Phys. Lett.* **94**, 162504 (2009).

¹²T. Marukame, T. Ishikawa, T. Taira, K.-i. Matsuda, T. Uemura, and M. Yamamoto, *Phys. Rev. B* **81**, 134432 (2010).

¹³W. Wang, E. Liu, M. Kodzuka, H. Sukegawa, M. Wojcik, E. Jedryka, G. H. Wu, K. Inomata, S. Mitani, and K. Hono, *Phys. Rev. B* **81**, 140402(R) (2010).

¹⁴H.-x. Liu, T. Kawami, K. Moges, T. Uemura, M. Yamamoto, F. Shi, and P. M. Voyles, *J. Phys. D: Appl. Phys.* **48**, 164001 (2015).

¹⁵K. Moges, Y. Honda, H.-x. Liu, T. Uemura, M. Yamamoto, Y. Miura, and M. Shirai, *Phys. Rev. B* **93**, 134403 (2016).

¹⁶B. Hu, K. Moges, Y. Honda, H.-x. Liu, T. Uemura, M. Yamamoto, J. Inoue, and M. Shirai, *Phys. Rev. B* **94**, 094428 (2016).

¹⁷K. Yakushiji, K. Saito, S. Mitani, K. Takahashi, Y. K. Takahashi, and K. Hono, *Appl. Phys. Lett.* **88**, 222504 (2006).

¹⁸T. Furubayashi, K. Kodama, H. Sukegawa, Y. K. Takahashi, K. Inomata, and K. Hono, *Appl. Phys. Lett.* **93**, 122507 (2008).

¹⁹Y. Sakuraba, K. Izumi, T. Iwase, S. Bosu, K. Saito, K. Takahashi, Y. Miura, K. Futatsukawa, K. Abe, and M. Shirai, *Phys. Rev. B* **82**, 094444 (2010).

²⁰T. Furubayashi, K. Kodama, T. M. Nakatani, H. Sukegawa, Y. K. Takahashi, K. Inomata, and K. Hono, *J. Appl. Phys.* **107**, 113917 (2010).

- ²¹N. Hase, T. M. Nakatani, S. Kasai, Y. K. Takahashi, and K. Hono, *J. Appl. Phys.* **109**, 07E112 (2011).
- ²²H. S. Goripati, M. Hayashi, T. Furubayashi, T. Taniguchi, H. Sukegawa, Y. K. Takahashi, and K. Hono, *J. Appl. Phys.* **110**, 123914 (2011).
- ²³Y. Sakuraba, K. Izumi, S. Bosu, K. Saito, and K. Takanashi, *J. Phys. D: Appl. Phys.* **44**, 064009 (2011).
- ²⁴Y. Sakuraba, M. Ueda, Y. Miura, K. Sato, S. Bosu, K. Saito, M. Shirai, T. J. Konno, and K. Takanashi, *Appl. Phys. Lett.* **101**, 252408 (2012).
- ²⁵H. Narisawa, T. Kubota, and K. Takanashi, *Appl. Phys. Express* **8**, 063008 (2015).
- ²⁶Y. Du, T. Furubayashi, T. T. Sasaki, Y. Sakuraba, Y. K. Takahashi, and K. Hono, *Appl. Phys. Lett.* **107**, 112405 (2015).
- ²⁷J. W. Jung, Y. Sakuraba, T. T. Sasaki, Y. Miura, and K. Hono, *Appl. Phys. Lett.* **108**, 102408 (2016).
- ²⁸S. Li, Y. K. Takahashi, Y. Sakuraba, N. Tsuji, H. Tajiri, Y. Miura, J. Chen, T. Furubayashi, and K. Hono, *Appl. Phys. Lett.* **108**, 122404 (2016).
- ²⁹T. Akiho, J. Shan, H.-x. Liu, K.-i. Matsuda, M. Yamamoto, and T. Uemura, *Phys. Rev. B* **87**, 235205 (2013).
- ³⁰P. Bruski, Y. Manzke, R. Farshchi, O. Brandt, J. Herfort, and M. Ramsteiner, *Appl. Phys. Lett.* **103**, 052406 (2013).
- ³¹T. Saito, N. Tezuka, M. Matsuura, and S. Sugimoto, *Appl. Phys. Express* **6**, 103006 (2013).
- ³²Y. Ebina, T. Akiho, H.-x. Liu, M. Yamamoto, and T. Uemura, *Appl. Phys. Lett.* **104**, 172405 (2014).
- ³³T. Uemura, T. Akiho, Y. Ebina, and M. Yamamoto, *Phys. Rev. B* **91**, 140410(R) (2015).
- ³⁴J. Kübler, A. R. Williams, and C. B. Sommers, *Phys. Rev. B* **28**, 1745 (1983).
- ³⁵S. Ishida, S. Fujii, S. Kashiwagi, and S. Asano, *J. Phys. Soc. Jpn.* **64**, 2152 (1995).
- ³⁶S. Picozzi, A. Continenza, and A. J. Freeman, *Phys. Rev. B* **66**, 094421 (2002).
- ³⁷I. Galanakis, P. H. Dederichs, and N. Papanikolaou, *Phys. Rev. B* **66**, 174429 (2002).
- ³⁸P. J. Webster, *J. Phys. Chem. Solids* **32**, 1221 (1971).
- ³⁹S. Picozzi, A. Continenza, and A. J. Freeman, *Phys. Rev. B* **69**, 094423 (2004).
- ⁴⁰J.-P. Wüstenberg, R. Fetzter, M. Aeschlimann, M. Cinchetti, J. Minár, J. Braun, H. Ebert, T. Ishikawa, T. Uemura, and M. Yamamoto, *Phys. Rev. B* **85**, 064407 (2012).
- ⁴¹D. Asakura, T. Koide, S. Yamamoto, K. Tsuchiya, T. Shioya, K. Amemiya, V. R. Singh, T. Kataoka, Y. Yamazaki, Y. Sakamoto, A. Fujimori, T. Taira, and M. Yamamoto, *Phys. Rev. B* **82**, 184419 (2010).
- ⁴²V. R. Singh, V. K. Verma, K. Ishigami, G. Shibata, T. Kadono, A. Fujimori, D. Asakura, T. Koide, Y. Miura, M. Shirai, G.-f. Li, T. Taira, and M. Yamamoto, *Phys. Rev. B* **86**, 144412 (2012).
- ⁴³V. R. Singh, V. K. Verma, K. Ishigami, G. Shibata, A. Fujimori, T. Koide, Y. Miura, M. Shirai, T. Ishikawa, G.-f. Li, and M. Yamamoto, *J. Appl. Phys.* **117**, 203901 (2015).
- ⁴⁴S. Ouardi, G. H. Fecher, S. Chadov, B. Balke, X. Kozina, C. Felser, T. Taira, and M. Yamamoto, *Appl. Phys. A: Mater. Sci. Process.* **111**, 395 (2013).
- ⁴⁵X. Kozina, J. Karel, S. Ouardi, S. Chadov, G. H. Fecher, C. Felser, G. Stryganyuk, B. Balke, T. Ishikawa, T. Uemura, M. Yamamoto, E. Ikenaga, S. Ueda, and K. Kobayashi, *Phys. Rev. B* **89**, 125116 (2014).
- ⁴⁶R. Fetzter, S. Ouardi, Y. Honda, H.-x. Liu, S. Chadov, B. Balke, S. Ueda, M. Suzuki, T. Uemura, M. Yamamoto, M. Aeschlimann, M. Cinchetti, G. H. Fecher, and C. Felser, *J. Phys. D: Appl. Phys.* **48**, 164002 (2015).
- ⁴⁷T. Valet and A. Fert, *Phys. Rev. B* **48**, 7099 (1993).